Int. J. Electrochem. Sci., 10 **(2015)** 7103 - 7110

International Journal of
ELECTROCHEMICAL
SCIENCE
www.electrochemsci.org

Fabrication and Characterization of $ZnFe_2O_4$/ZnO Based Anticorrosion Pigments

N. M. Deraz[1,*], *Omar H. Abd-Elkader*[2, 3]

[1]Physical Chemistry Department, Laboratory of Surface Chemistry and Catalysis, National Research Centre, Dokki, Cairo 12622, Egypt
[2]Zoology Department, College of Science, King Saud University, Riyadh 11451, Kingdom of Saudi Arabia
[3]Electron Microscope and Thin Films Department, National Research Center (NRC), El- Behooth Street, 12622, Giza, Egypt
[*]E-mail: nmderaz@yahoo.com

Received: 25 December 2014 / *Accepted:* 5 July 2015 / *Published:* 28 July 2015

Reassured combustion route used for synthesized nanocomposite $ZnFe_2O_4$/ZnO by polyethylene glycol (PEG). The degree of crystallinity and the nanoparticle size determined via X-ray diffraction technique. Morphology and composition fully considered via Scanning Electron Microscope (SEM) and Energy Dispersive Spectrometry (EDS) techniques. Vibrating sample magnetometer (VSM) deliberate the magnetic properties. Both the saturation magnetization (30 emu/g) and the remnant magnetization (8 emu/g) found depending on the size of constituents of the composite studied. PEG relieved combustion method brought about formation of moderate crystalline $ZnFe_2O_4$/ZnO nanocomposite.

Keywords: XRD; SEM, EDX; M_s, $ZnFe_2O_4$/ZnO.

1. INTRODUCTION

Nanomaterials are cornerstones of nanoscience and nanotechnology they have broad and interdisciplinary area of research and development activity. It has the potential for revolutionizing of the physical and chemical properties such as a unique magnetic properties, electrical conductivity, optical energy gap, refractive index and uppermost mechanical properties. So, these materials used in different fields such as microwave absorbers and catalysis, electronic ignition systems, inductor core, transformer circuits, recording equipment, telecommunications, magnetic fluids and sensors , [1-3]. In fact, ferrite based nanoparticles show unusual magnetic properties such as single-domain behavior and superparamagnetism [4, 5]. These properties not remarked in bulk ferrites. The chemical compositions

and the preparation routes controlled in different properties of the ferrite materials. Thus, the most important factor in the design and preparation of ferrite materials is the chemical aspect.

The spinel group contains over twenty members, but only a few are considered common. The general formula of the spinel group is AB_2O_4, $ZnFe_2O_4$, are a class of semiconductors with narrow bandgaps, present characteristics of favorable magnetism ,excellent visible-light response, good and photochemical stability [6, 7]. Due to the lower valence band potential and poor property in photoelectric conversion the superior properties of zinc ferrite, using this ferrite in photocatalysis is limited [8]. To open the use of zinc ferrite in photocatalysis, it must mixed another oxide such as ZnO. High, chemical stability, environmental friendly and morphology controllable preparation, Nano ZnO widely used as photocatalysts [9]. Various techniques used for preparation of nanomagnetic materials [10-13]. Among these techniques, combustion method has a good sound due to its simple preparation, chemical homogeneity, fast production rate and inexpensive raw materials [14]. Using glycine assisted combustion method pure and doped zinc ferrites is prepared [14]. This method resulted in formation of single spinel zinc ferrite phase can doping with different cations brought about a considerable alteration in the morphological, structural and magnetic properties of zinc ferrite [14].

Some investigators reported using of polyethylene glycol (PEG) in the combustion method led to promising results in diversiform oxides/ferrites in a single step [15]. These authors have some of the possible reasons for employing PEG in the combustion method. These reasons are: (i) PEG have a low decomposition temperature because its melting point is 62°C. (ii) Accordingly its melting nitrate precursors dispersed in the molten polyethylene glycol (iii) PEG renowned as a dispersant and good surfactant. (v) With precursors PEG burns in air exothermically to construct desired ultrafine and nano metal oxides/ferrites [15]. Preliminary experiments for employing small amount of PEG show formation of $ZnFe_2O_4$/ZnO nanocomposite. Thus, the aim to prepare of $ZnFe_2O_4$/ZnO nanocomposite higher surface, Nano-catalysts have exceptional surface activity achieved using PEG as fuel.

In addition, the spinel based ferrites used as pigments in coatings due to their higher anticorrosion efficiency at higher temperatures and aggressive environments. Ferrites containing Zn^{2+} cations, display properties needs for anticorrosion pigments in paints [16]. Zinc ferrite established anticorrosion pigments suitable for epoxy solvent-borne binders and water-borne application [17]. Contrastive forms ferrites such as films, sheets, ceramic tiles, paints, and powders can absorb variably electromagnetic radiation in microwave bands cast.

Consequently, this study aims to prepare $ZnFe_2O_4$/ZnO nanocomposite using polyethylene glycol assisted combustion method. The structural, morphological and magnetic properties of the $ZnFe_2O_4$/ZnO nanocomposite determined. The techniques employed were XRD, SEM, EDX and VSM.

2. EXPERIMENTAL

2.1. Materials

Calculated parts of zinc and iron nitrates with some of polyethylene glycol (PEG) used to prepare Iron/zinc mixed oxides. The mixed precursors concentrated in a porcelain crucible heated to

400 ^{o}C for quarter hour on a hot plate. When a crucible temperature reached, crystal water gradually vaporized during, much foams produced and spark appeared at one corner, yielding a voluminous and fluffy product in the container. To hold wished powder final product is milled by a gate mortar. The chemicals employed in the present work supplied by Prolabo Company.

2.2. Techniques

XRD measurements used to determine the compositions of the ZnFe2O4/ZnO nanocomposite. An X Pert Pro diffractometer using Cu-Kα radiation at 40 kV and 40 mA. The scans were typically performed over a 2θ range of 4–100 at a speed of 2θ of 2 ° min^{-1}.

The crystallite sizes of $ZnFe_2O_4$ and ZnO involved in the researched solid established on X-ray diffraction line broadening by using Scherrer equation [18].

$$d = \frac{B\lambda}{\beta \cos\theta}$$

Where d , β, 2θ, and λ are the average crystallite size of the phase under investigation, the full-width at half maximum of the peaks in radians, diffraction angle in radians, and the wavelength of the X-rays in nanometers is, Structural parameters such as the distance between the magnetic ions (L_A and L_B), ionic radii (r_A, r_B) and bond lengths (A–O and B–O) on tetrahedral (A) sites and octahedral (B) sites of cubic spinel structure for the produced zinc ferrite crystallites determined from XRD measurement.

Scanning electron micrograph (SEM) observed on high-performance, high resolution of 3.0nm JSM-6380 .Energy dispersive X-ray analysis (EDX) carried out JSM-6380 LA with an attached kevex Delta system. To stimulate the emission of characteristic X-rays from a specimen, a high-energy beam of charged particles is focused into the sample using accelerating voltage 20 KV, accumulation time 100s, window width 8 μm. The surface molar composition determined by the Asa method, Zaf-correction, Gaussian approximation.

The magnetic properties of the examined solids measured at room temperature using a vibrating sample magnetometer (VSM; 9600-1 LDJ, USA) in a maximum applied field of 15 k Oe. From the obtained hysteresis loops, the saturation magnetization (M_s), remanence magnetization (M_r) and coercivity (H_c) determined.

3. RESULTS AND DISCUSSION

3.1. XRD analysis

Figure 1 showed the XRD pattern of as prepared sample consisted of nano-crystalline $ZnFe_2O_4$ and ZnO particles, contain moderate diffraction lines coincide with the standard data of the cubic spinel $ZnFe_2O_4$ (Franklinite) and ZnO (Zincite) phases with the *Fd3m* and *P63mc* space groups (PDF No. 74-2397 and 5-664), respectively. The peaks of the as prepared solid indexed to the crystal plane

of spinel Zn ferrite (220), (311), (222), (400), (422), (511), (440), (620), (533) and (622) and the crystal planes of ZnO (100), (002), (101), (102), (110), (103) and (112), respectively. The crystallite sizes of $ZnFe_2O_4$ and ZnO estimated about 35 nm and 33 nm from the peak broadening of the (311) and (101) peaks, respectively, using Scherer's equation.

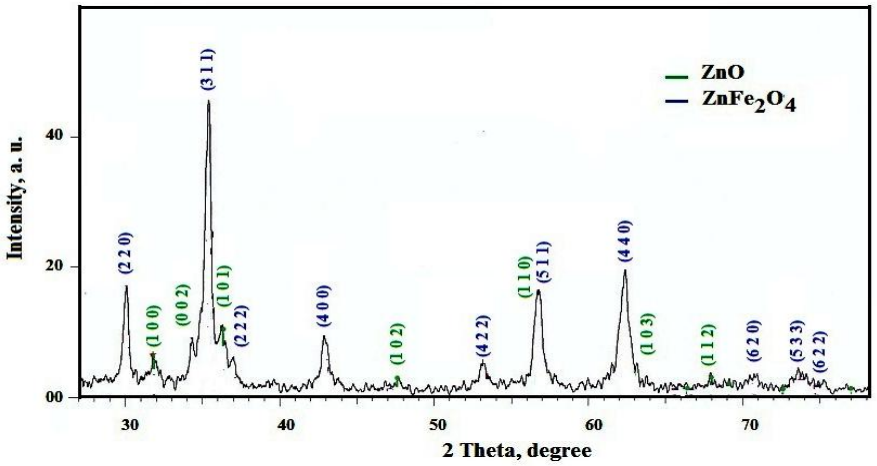

Figure 1. XRD pattern for the as prepared nanocomposite.

From that data different structural parameters of both $ZnFe_2O_4$ and ZnO such as the lattice constant (a), unit cell volume (V), X-ray density (D_x) calculated and listed in Table1.

Table 1. Structural parameters for ZnO and $ZnFe_2O_4$ involved in the as prepared nanocomposite.

Elements	Crystallite size (Surface)	a (nm)	V (nm^3)	D_x
ZnO	**33**	**0.3249**	**0.4758**	**5.68**
$ZnFe_2O_4$	**35**	**0.8414**	**0.5957**	**5.37**

The calculated values of a, L_A, L_B , r_A, r_B, A–O and B–O of Zn ferrite are 0.3643, 0.2975, 0.0574, 0.0695, 0.1924 and 0.2045 nm, respectively.

3.2. SEM measurement

Figure. 2. displays SEM micrograph of as-prepared powder forming spongy and fragile zinc ferrite. The fracture surfaces of the collected powders formed by using PEG. In addition, the as synthesized sample consisted of multigrain agglomerations. One can see voids and pores in the sample. This observation could assigned to the release of large amount gases during combustion due retrogradation of PEG and metal nitrates.

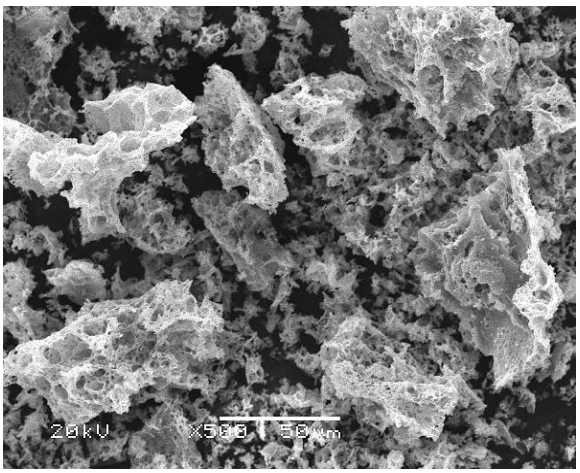

Figure 2. SEM image for the as prepared nanocomposite.

3.3. EDX analysis

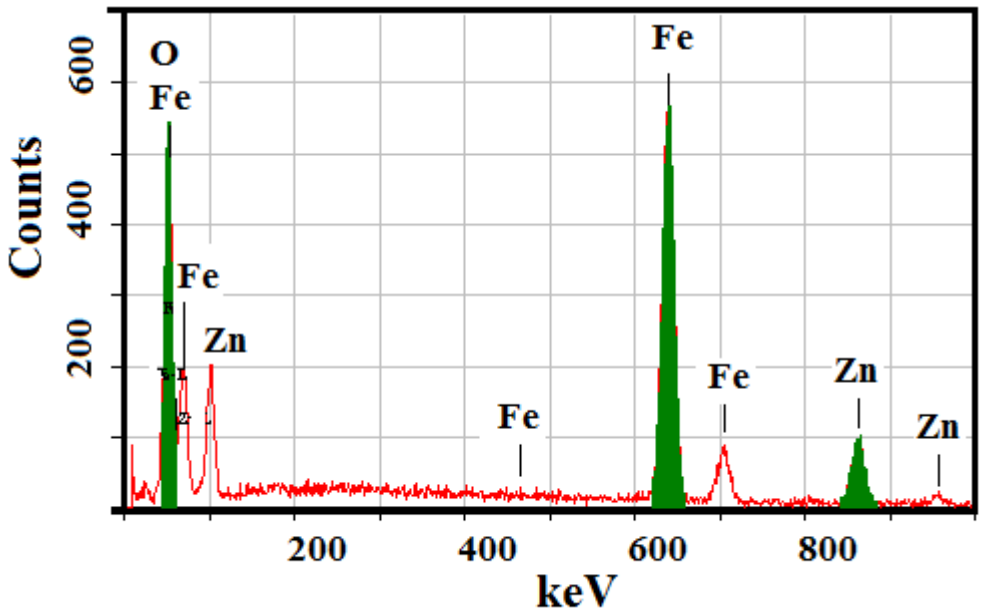

Figure 3. EDX pattren for the as prepared nanocomposite.

Energy dispersive X-ray (EDX) analysis of the as prepared specimen was carried out at 20kV on the surface of solid as shown in Fig. 3. The concentrations of the detected elements tabulated in Table 2. It can see from this table the surface Zn concentration is lower than bulk zinc concentration. Opposite behavior observed with iron species. The concentrations of iron species are higher than that of zinc species. In pure ZnO compound zinc content is 80.34%, thus the product purity can be calculated depending upon EDX data in Table 2. It was found the purity of zinc is 39.39%. This result shows that impurities exist suiting to extra reflections related to $ZnFe_2O_4$ as shown in Fig. 1.

Table 2. The atomic abundance of elements measured at 20 keV and different points over the as prepared sample.

Elements	Found (Surface)	Calculated (Bulk)	Surface Fe/Zn ratio	Bulk Fe/Zn ratio
O	21.50	26.44	2.32	1.71
Zn	23.61	46.33		
Fe	54.89	27.12		

In addition, the bulk Fe/Zn ratio is 1.71 less than the surface Fe/Zn ratio that is 2.32. This suggests populating iron species at the surface layers. However, the iron and zinc species involved in zinc ferrite preferred the octahedral and tetrahedral sites, respectively [14]. Also, the octahedral site more exposed to the surface layer. These findings resulted in the speculation presented in Fig. 4. This figure showed that ZnO particle coated by $ZnFe_2O_4$ particles.

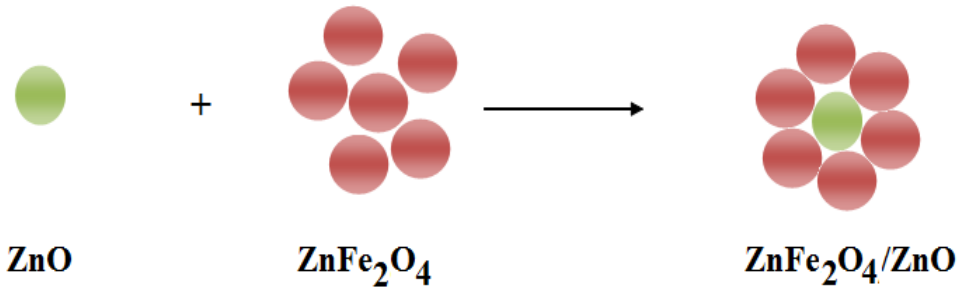

Figure 4. Scheme for formation of $ZnFe_2O_4$/ZnO nanocomposite.

3.4. Magnetic properties

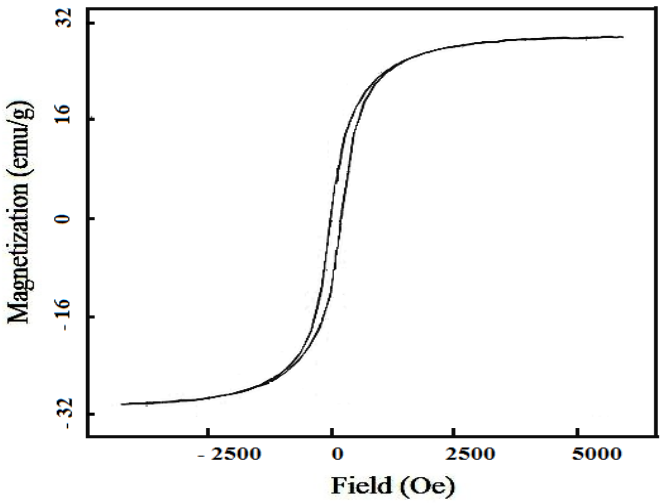

Figure 5. Magnetic hysteresis curve for the as prepared nanocomposite.

At room temperature, 15 KOe applied Magnetic Field the magnetic hysteresis loop of the as-prepared powders measured, restricted the saturation magnetization (Ms), remanent magnetization (Mr) and the coercivity (Hc) as shown as in fig. 5.

The M_S value found to be 30 emu/g and the value M_r was 8 emu/g for the $ZnFe_2O_4$ sample. The matching squareness ratio (M_r/M_s) found to be 0.267. In addition, the coercivity of the researched sample was found to 108 Oe. . It found the as-prepared Zn ferrite particles in this work presented a saturation magnetization lower than that of $ZnFe_2O_4$, prepared by glycine as fuel [14]. One author reported that glycine relieved preparation of zinc ferrite, with crystallite size of 62 nm, have the values of M_S, M_r, M_r/M_s and H_c are 52 emu/g, 15 emu/g, 0.289 emu/g and 46 Oe, respectively [14]. The decrease in the values of M_S, M_r, M_r/M_s of zinc ferrite prepared by PEG could attributed to the decrease in grain size and redistribution of cations with subsequent presence of separated nonmagnetic zinc oxide. On the other hand, this demeanor fulfil an increase in the non-collinear spin structure which originated from the pinning of the surface spins [19, 20]. In addition, the coercivity of $ZnFe_2O_4$/ZnO composite lower than $ZnFe_2O_4$. This observation clarified the magneto- crystalline anisotropy. The magneto- crystalline anisotropy is dependent on spreads magnetic moments of different ions on the surface of the nanoparticles [19, 20].

4. CONCLUSIONS

PEG assisted combustion method resulted formation of nano-scale size $ZnFe_2O_4$/ZnO nanocomposite with moderate homogeneously distributed crystalline particles. Zn ferrite obtained using PEG as fuel has (108 Oe) coercivity values and (30 emu/g) moderate saturation magnetization. These values are lower than nano-magnetic Zn ferrite materials prepared by using glycine.

ACKNOWLEDGEMENT
This project was supported by King Saud University, Deanship of Scientific Research, College of Science Research Centre.

References

1. M.A. Willard, L.K. Kurihara, E.E. Carpenter, S. Calvin, V.G. Harris, *Int. Mater. Rev*. 49 (2004) 125.
2. O.S. Mathew, R.S. Jiang, *Chem. Eng. J*. 129 (2007) 51.
3. B. Reddy, T. Sivasankar, M. Sivakumar, V. Moholkar, *Ultrason. Sonochem*. 17(2010) 416.
4. D. L. Leslie-Pelecky and R. D. Rieke, *Chem. Mater.* 8(1996)1770.
5. C. K. Lim, Y. S. Kim, N. Y. Park, and J. Lee, *IEEE Trans. Magn.* 41(2005)2670.
6. X.Y. Li, Y. Hou, Q.D. Zhao, W. Teng, X.J. Hu, G.H. Chen, *Chemosphere* 82 (2011)581.
7. P. Laokul, V. Amornkitbamrung, S. Seraphin, S. Maensiri, *Curr. Appl. Phys*. 11(2011) 101.
8. S.H. Xu, D.L. Feng, W.F. Shangguan, *J. Phys. Chem*. C 113 (2009) 2463.
9. L.P. Xu, Y.L. Hu, C. Pelligra, C.H. Chen, L. Jin, H. Huang, S. Sithambaram, M.M.J.L. de Vilades, A. Lopez-Delgado, E. Vila, *J. Alloys Compd*. 287 (1999) 276.
10. J. Jin, T. Bai, X. Chang, B. Bai, *Chem. Res. Appl*. 13 (2001) 667.
11. S. Yu, T. Fujino, M. Yoshimura, *J. Magn. Magn. Mater*. 256 (2003) 420.

12. I. Mohai, J. Szepvolgyi, I. Bertoti, M. Mohai, J. Gubicza, T. Ungar, *Solid State Ionics*141/142 (2001) 163.
13. H. Yang, X. Zhang, C. Huang, W. Yang, G. Qiu, *J. Phys. Chem. Solids* 65 (2004)1329.
14. N. M. Deraz, *J. Anal. Appl. Pyrolysis* 91 (2011) 48.
15. S.Basavaraja, H. Vijayanand, A. Venkataraman, U. P. Deshpande, T. Shripathi, *Synth. React. Inorg. Met-Org. Nano-Metal Chem.* 37(2007) 409.
16. A.U. Chaudhry, Rahul Bhola, Vikas Mittal, Brajendra Mishra, *Int. J. Electrochem. Sci*., 9 (2014) 4478.
17. Andréa Kalendová, Miroslav Ulbrich, Petr Kalenda, CSc, *Transfer inovácií* 17(2010)68.
18. B. D. Cullity, Elements of X-ray Diffraction, Addison-Wesly Publishing Co. Inc. 1976 (Chapter 14).
19. M. Caizer, Stefanescu, *J. Phys. D: Appl. Phys*. 35 (2002) 3035.
20. R.H. Kodama, A.E. Berkowitz, E.J. Mcniff, S. Foner, *Phys. Rev. Lett*. 77 (1996) 394.